Breaking reciprocity by designed loss

Journal of the Optical Society of America B
OPTICAL PHYSICS

Breaking reciprocity by designed loss

I. Peshko,[1] D. Pustakhod,[2] and D. Mogilevtsev[1,*]

[1]B. I. Stepanov Institute of Physics, National Academy of Sciences of Belarus, Nezavisimosti Ave. 68, Minsk, 220072, Belarus
[2]Eindhoven Hendrik Casimir Institute (EHCI), Eindhoven University of Technology, 5600 MB, Eindhoven, The Netherlands
*Corresponding author: d.mogilevtsev@ifanbel.bas-net.by

Received 6 April 2022; revised 24 May 2022; accepted 5 June 2022; posted 8 June 2022; published 24 June 2022

In this paper, we show how designed loss in open quantum systems can break the reciprocity of field propagation, and how non-reciprocal and even unidirectional propagation can be achieved for different kinds of designed loss, both linear and nonlinear. In particular, we show how unidirectional propagation can be achieved for input states of certain symmetry in linear schemes, and demonstrate the possibility of building a single-mode optical insulator by combining two kinds of nonlinear designed losses, and the way to build a non-reciprocal asymmetric field distributor with a planar structure of dissipatively coupled waveguides. We discuss the feasibility of the considered schemes and suggest possible realizations.

https://doi.org/10.1364/JOSAB.460706

1. INTRODUCTION

Recently, non-reciprocal propagation of the electromagnetic field became a popular research theme. Non-reciprocity is important for quite a wide range of practical tasks, from field distributors and circulators to lasing and high-precision sensing [1–6]. Current interest for realization of non-reciprocal systems, and especially isolators, is born of the necessity to extend methods commonly applied for longer wavelengths (radio, microwaves, etc.) toward the optical region and the possibility of integrating non-reciprocal systems into photonic circuitry. Traditional realizations implementing magneto-sensitive media are either hard to realize on the basis of existing integration platforms or difficult even to realize for optical wavelength, or both [4,5]. So, a plethora of novel schemes for breaking reciprocity has appeared in recent years. There are schemes exploiting time modulation [7,8], nonlinearities [9–11], and interaction with few-level systems, such as atom-like structures [4,12–14], optomechanics [15], and topological properties of structured media [5,16,17].

Some quite interesting results were also obtained by considering loss. Recently, it was shown that even common single-photon energy losses in conjunction with the usual (i.e., unitary) coupling can also be a tool for devising non-reciprocal multi-mode structures [18,19]. Even more interesting results are obtained with designed loss, i.e., for example, when different systems are coupled to the same loss reservoir inducing dissipative coupling between them, or when loss is made to be nonlinear. For instance, designed collective linear loss can lead to unidirectional transport and amplification [20,21].

Here we present another interesting feature of designed loss: its ability to break reciprocity in photonic systems without conjoining with simultaneous unitary coupling. We discuss a way to do this with the designed loss, provide several examples, and outline ways for possible practical realizations, in particular, with integrable planar waveguide systems. Notice that schemes relying only on the designed loss might be easier to realize in practice than schemes combining unitary and dissipative couplings, since one does not need to adjust different types of couplings. We show how the designed nonlinear loss can break reciprocity even for a single-mode system, and how to realize this system using conventional Kerr nonlinearity and dissipative coupling. We also demonstrate the way to achieve non-reciprocal asymmetric field distribution between waveguides using dissipative coupling.

The outline of the paper is as follows. In Section 2, we recall a non-reciprocity criterion for linear systems and suggest a simple generalization of the reciprocity concept suitable for quantum state/correlation transfer, since nonlinear designed loss can produce non-classical states from classical input. Then, in Section 3, we describe the mechanics of reciprocity breaking for dissipatively coupled systems and give examples of two-mode devices, providing for asymmetric transfer between waveguides in different directions. In Sections 4 and 5, we discuss examples of single-mode reciprocity breaking and unidirectional propagation with nonlinear designed loss in asymptotic and non-asymptotic regimes, and address practical realization of such schemes. We argue that such schemes are quite feasible with existing photonic integration platforms and with such common modeling and simulation tools as systems of laser-written waveguides in bulk dielectric. In Section 6, we show how such a common type of loss as dephasing can also break reciprocity, and demonstrate reciprocity breaking in correlation propagation for a simple device of a beam splitter and dephaser. In Section 7, we discuss a non-reciprocal field distributor with

sharply asymmetric field exchange between waveguides, implementing only dissipative coupling. In Appendices A and B, we describe several designs of integrable dissipatively coupled structures and discuss how dissipative coupling arises from the system of unitary coupled waveguides with designed loss.

2. RECIPROCITY

First, let us clarify the concept of reciprocity and its breaking as applicable for the designed loss structures. We consider here both linear and nonlinear structures, and the latter are known to produce non-classical states from classical ones [22–25]. So, it is necessary to provide for a suitable generalization of the reciprocity concept for open quantum systems. Here we will not pursue the task of discussing the general reciprocity concept for open quantum systems in the manner as it was done for unitary systems, for example, in Refs. [26,27]. Here we introduce a simple generalization of the classical definition [4,26–29]). We formulate the classical definition using quantum operators in the following way [30,31]. Let us define a set of N input modes described by the bosonic annihilation operators $\vec{a} = [a_1, a_2, \ldots a_N]$ (and the corresponding creation operators $a_n^\dagger$), and a set of N output modes described by the bosonic annihilation operators $\vec{b} = [b_1, b_2, \ldots b_N]$ (and the corresponding creation operators $b_n^\dagger$). For the linear device transforming input into output, one can write [30]

$$\vec{b} = \mathbf{S}\vec{a} + \vec{N}, \tag{1}$$

where the vector of operators $\vec{N}$ describes noise. For passive systems with $\langle \vec{N} \rangle = 0$, one gets

$$\langle \vec{b} \rangle = \mathbf{S}\langle \vec{a} \rangle, \tag{2}$$

where the expression $\langle x \rangle = Tr\{x\rho\}$ denotes the quantum mechanical average of operator x over density matrix ρ describing the quantum state of the whole system. For coherent modal states, $\langle \vec{a} \rangle$, $\langle \vec{b} \rangle$ are the modal amplitudes. Thus, one arrives to the well-known classical description of reciprocity for the system of electromagnetic field modes. Reciprocity is directly associated with the features of scattering matrix $\mathbf{S}$. Non-symmetrical scattering matrix $\mathbf{S} \neq \mathbf{S}^T$ means that the system breaks reciprocity [4,26–29]. Notice that symmetry should be considered taking into account the arbitrariness of the modal phase, i.e., the possibility to make all elements of the scattering matrix real by the local gauge transformation

$$x \to x \exp\{i\phi_x\}, \tag{3}$$

where $x = a, b$ with some phases ϕ_x [18].

Generally, Eq. (1) allows extending the description of reciprocity for the quantum case. For example, one can derive the transfer equation similar to Eq. (2) also for the correlation function of different orders. For nonlinear transformations, Eq. (1) can hardly be applied. However, one can return to linearity just by considering transformation of the density matrix elements instead of modal operators. Let us proceed discussing reciprocity in open quantum systems in such a way as it was done for unitary systems in Refs. [26,27].

Let us assume that our system of interest is described by density matrix ρ_{in}, and we have two propagators describing propagation in different directions, $\overleftarrow{\mathcal{D}}$ and $\overrightarrow{\mathcal{D}}$. The state transformation corresponding to propagation in these directions is described by the mapping

$$\rho_{\text{in}} \to \overrightarrow{\rho}_{\text{out}} = \overrightarrow{\mathcal{D}}\rho_{\text{in}}, \quad \rho_{\text{in}} \to \overleftarrow{\rho}_{\text{out}} = \overleftarrow{\mathcal{D}}\rho_{\text{in}}. \tag{4}$$

Here we are not interested in the complete description of the transferred density matrix but rather in the dynamics of certain observable quantities, for example, energy. If for the same input state of our passive system the output energy for different propagation directions is different, it is a sufficient condition of reciprocity breaking. So, let us introduce a set of Hermitian operators P_j describing the observables of interest, so that quantities $p_j = Tr\{P_j\rho_{\text{in}}\}$, $\overrightarrow{p}_j = Tr\{P_j\overrightarrow{\rho}_{\text{out}}\}$ ($\overleftarrow{p}_j = Tr\{P_j\overleftarrow{\rho}_{\text{out}}\}$) can be measured at the input and output of our device described by map $\overrightarrow{\mathcal{D}}$ ($\overleftarrow{\mathcal{D}}$). For reciprocal transmission, one would have

$$\overleftarrow{p}_j = \overrightarrow{p}_j, \quad \forall\, j. \tag{5}$$

Thus, breaking Eq. (5) would mean non-reciprocity. Notice that this simple equation implies a number of important observations. First, the condition in Eq. (5) is state dependent. So, one needs to define a class of initial density matrices $\{\rho_{\text{in}}\}$ to discuss reciprocity. Second, reciprocity is defined for a particular set of $\{P_j\}$. This set might be complete and sufficient for description/inference of the density matrix, or not. Different sets of $\{P_j\}$ might demonstrate both reciprocity and breaking of it for the same system. Only proving reciprocity for arbitrary initial states and observables allows calling the system completely reciprocal.

3. BREAKING RECIPROCITY BY LINEAR DISSIPATIVE COUPLING

First, let us demonstrate how a purely dissipative device breaks reciprocity. We consider a set of dissipatively coupled waveguides without additional unitary coupling between them. Such a coupling can be realized by the usual unitary coupling of several waveguides to the common dissipative reservoir, say, a waveguide with strong loss [as depicted in Fig. 1(a)]. Such an arrangement can be easily realized in practice, for example, by laser-writing a system of single-mode waveguides in a bulk glass [24,25,32–34], or growing planar semiconductor structures on some platform, for example, InGaAsP material on InP [6,35] (see Appendix A for a discussion of several designs of dissipative waveguide couplers on the integrated photonic platform).

To demonstrate a breaking of reciprocity, let us consider a bipartite two-waveguide system as schematically shown in Fig. 1(c). During propagation through the jth part of the system, the density matrix ρ dynamics is described by the following master equation:

$$\frac{d}{dt}\rho = \gamma_j\left(2L_j\rho L_j^\dagger - \rho L_j^\dagger L_j - L_j^\dagger L_j\rho\right), \tag{6}$$

where the Lindblad operators for the jth part are taken as $L_j = a + \delta_j b$, a and b being the annihilation operators for modes A and B; δ_j are asymmetry parameters describing the respective strength of waveguides coupling to the common reservoir; γ_j are decay rates corresponding to each part. Taking into account a possibility of the local gauge transformation,

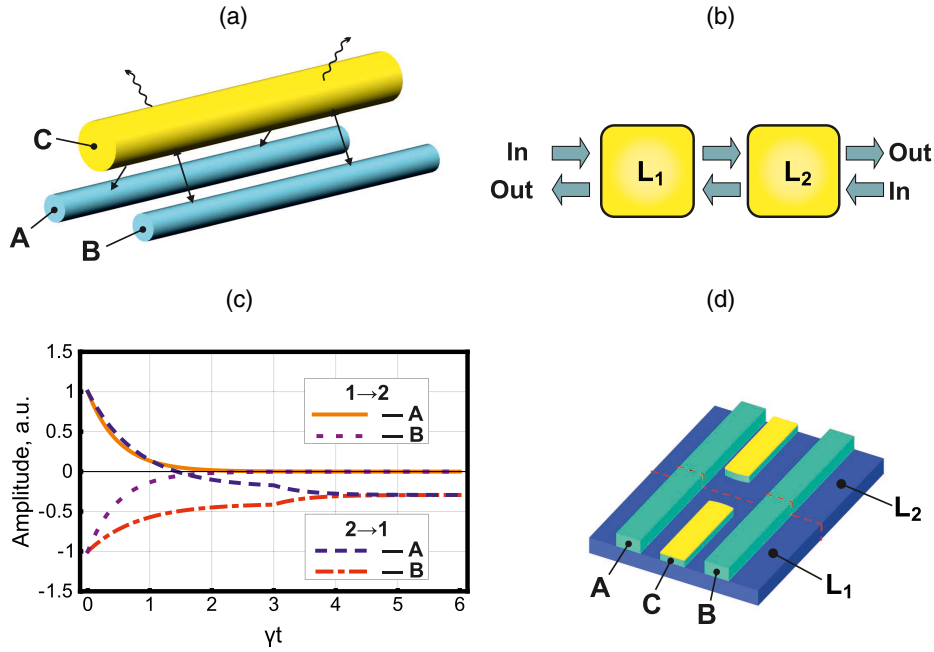

Fig. 1. (a) Scheme of the dissipative coupling of two waveguides A and B through the common loss reservoir are represented as lossy waveguide C. (b) Illustration of the modal amplitude dynamics for direct and reverse propagation through the two waveguides with different dissipative couplings in the first part [denoted as L_1 in (c)] and second part [denoted as L_2 in (c)]. Solid and dotted curves correspond to field propagation in waveguides A and B in direction $1 \to 2$, and dashed and dashed-dotted lines correspond to field propagation in waveguides A and B in direction $2 \to 1$, respectively. For the first device part, the Lindblad operator is $L_1 = \gamma(a - 0.5b)$, and for the second part, the Lindblad operator is $L_2 = \gamma(a - b)$. The initial amplitude for mode a is $+1$, and for mode b -1. (d) Scheme of the integrable device combining two kinds of dissipative coupling by variable placing of a central lossy waveguide between two low-loss waveguides (see discussion in Appendix A).

Eq. (3), one can assume real δ_j (this we also assume in the further considerations). In Appendix B, we show how master Eq. (14) arises in the system of single-mode waveguides illustrated in Fig. 1(a).

In Fig. 1(b), one can see an illustration of reciprocity breaking for bipartite systems with $L_1 = \gamma(a - 0.5b)$ and $L_2 = \gamma(a - b)$. For the asymmetric input state of both modes (i.e., when the sum of the amplitudes is zero), one has unidirectional energy flow through the system. For such input, the action of the second part of the device just exponentially reduces the state to the vacuum.

Such behavior can be easily understood from the character of dynamics dictated by master Eq. (6). The dissipative coupling between modes in the jth part of the system drives their state to the one satisfying $L_j\rho = 0$ [24,34]. Asymptotically (i.e., for interaction time tending to infinity), the modal amplitude transformation can be described by the following scattering matrix:

$$\begin{bmatrix} \langle a_{\rm out}\rangle \\ \langle b_{\rm out}\rangle \end{bmatrix} = \mathbf{S}_j \begin{bmatrix} \langle a_{\rm in}\rangle \\ \langle b_{\rm in}\rangle \end{bmatrix}, \quad \mathbf{S}_j = \frac{1}{1+\delta_j^2}\begin{bmatrix} \delta_j^2 & -\delta_j \\ -\delta_j & 1 \end{bmatrix}. \tag{7}$$

Generally, for $\delta_1 \neq \delta_2$ and $\delta_1\delta_2 \neq -1$, the product of matrices $\mathbf{S}_1$ and $\mathbf{S}_2$ is not symmetric:

$$\mathbf{S}_1\mathbf{S}_2 = \frac{1+\delta_1\delta_2}{(1+\delta_1^2)(1+\delta_2^2)}\begin{bmatrix} \delta_1\delta_2 & -\delta_1 \\ -\delta_2 & 1 \end{bmatrix}. \tag{8}$$

So, our bipartite device is indeed not reciprocal. Moreover, it does not allow the states satisfying $\delta_1\langle a_{\rm in}\rangle - \langle b_{\rm in}\rangle = 0$ to propagate in direction $1 \to 2$, and it does not allow the states satisfying $\delta_2\langle a_{\rm in}\rangle - \langle b_{\rm in}\rangle = 0$ to propagate in the opposite direction. Notice that different dissipative couplings in the realization schematically depicted in Fig. 1(a) can be simply realized by adjusting coupling with the common reservoirs, for example, by adjusting distances between waveguides A and B and the central dissipative waveguide as shown in Fig. 1(d) [25,34].

Interestingly, the simple linear device discussed here can offer quite considerable asymmetry in energy exchange between waveguides for different propagation directions. Indeed, it is easy to get from Eq. (8) that the ratio of the off-diagonal elements of the matrix products,

$$\left|\frac{[\mathbf{S}_1\mathbf{S}_2]_{12}}{[\mathbf{S}_2\mathbf{S}_1]_{12}}\right| = \left|\frac{\delta_1}{\delta_2}\right|, \tag{9}$$

is proportional to the ratio of the asymmetry parameters. As long as the value of $\delta_j\gamma$ remains much larger than the rate of uncorrelated single-photon loss inevitably present in a realistic waveguide system, one can get $|\frac{\delta_1}{\delta_2}|^2$ difference in energy transmission between waveguides in different directions. For example, for the planar systems described in Appendix A, it seems realistic to reach the ratio of 0.1 between waveguide coupling rates in the scheme depicted in Fig. 1(d), thus to have $|\frac{\delta_1}{\delta_2}|^2 = 0.01$ and 20 dB in energy exchange asymmetry.

Naturally, our discussion can be easily extended for a more involved dissipatively coupled system of modes. The main message would be the same: conjunction of parts with different dissipative couplings leads to breaking of reciprocity.

Also, it is useful to note that breaking reciprocity can be achieved with only one of two parts being a dissipative coupler. Indeed, replacing, for example, the first part with the beam splitter transforming some set of input states to one satisfying $\delta_2\langle a_{\rm in}\rangle - \langle b_{\rm in}\rangle = 0$, one gets unidirectional propagation of energy for this set of states (only for $2 \to 1$). Also, to break reciprocity, one can simply introduce different uncorrelated losses in both modes of the first part. Indeed, for the uncorrelated loss in both waveguides A and B (taken to be finite length) the scattering matrix is $\mathbf{S}_1 = \mathrm{diag}\{T_A, T_B\}$, where T_A, T_B are transmission coefficients for modes A and B. We assume the asymptotic regime for the second, dissipative coupler part. So, for transmission through the bipartite compound device, one has the following scattering matrix:

$$\mathbf{S}_2\mathbf{S}_1 = \frac{1}{1+\delta_2^2}\begin{bmatrix} T_A\delta_2 & -T_B\delta_2 \\ -\delta_2 T_A & T_B \end{bmatrix}. \tag{10}$$

The product, Eq. (10), is asymmetric. The asymmetry in energy exchange between waveguides is therefore defined by the ratio $(T_A/T_B)^2$.

4. BREAKING RECIPROCITY WITH NONLINEAR DISSIPATION

The obvious idea of breaking commutativity of dynamics in different parts of a compound system to break reciprocity can be easily extended for the general dissipative dynamics. Generally, the state transformation of the open system can be described in a standard way with help of the Kraus operators D_j as

$$\rho_{\rm out} = \sum_{\forall j} D_j \rho_{\rm in} D_j^\dagger, \tag{11}$$

where the Kraus operators satisfy $\sum_{\forall j} D_j^\dagger D_j = 1$ [36].

It is easy to surmise that for our bipartite system as depicted in Fig. 1(c), non-commutativity of Kraus operators $D_j^{(1)}$ and $D_k^{(2)}$ corresponding to the first and second parts of the system, can also lead to breaking of reciprocity. Now let us show that the dissipative systems possessing several stationary states (similar to the linear case described above) can also break reciprocity. Moreover, in stark difference with the linear case, such a system can provide for single-mode non-reciprocity.

Indeed, let us consider a simple example of single-mode subsystems 1 and 2 with just two stationary states each. These systems are described by the following Kraus operators:

$$D_m^{(1,2)} = \begin{cases} |m_{1,2}\rangle\langle m| & \forall m \geq m_{1,2} \\ |0\rangle\langle m| & \forall m < m_{1,2}, \end{cases} \tag{12}$$

where states $|m\rangle$ are Fock states with m photons of the single considered mode, and $m_{1,2} \neq 0$. For $m_1 \neq m_2$, some Kraus operators corresponding to different parts are obviously not commuting, so the field propagation is not reciprocal. Moreover, a combination of subsystems 1 and 2 realizes a single-mode optical insulator. Indeed, for $m_1 > m_2$, any Fock-state input with $m > m_1$ produces a Fock state with m_2 photons when propagating $1 \to 2$, whereas any state input from the opposite side (i.e., when $2 \to 1$) produces just the vacuum state.

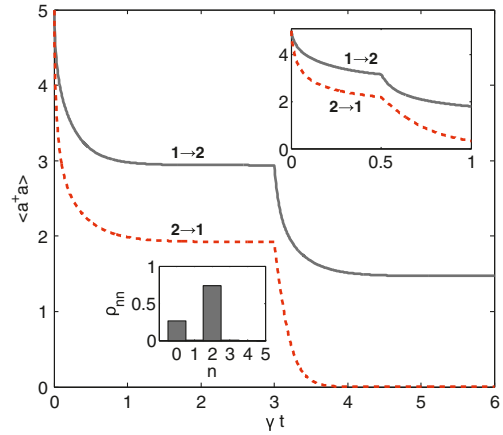

Fig. 2. Dynamics of the population for the single-mode bipartite system with parts described by the Lindblad operators, Eq. (13), with $m_1 = 4$ and $m_2 = 2$ as given by master Eq. (6) for the initial coherent state with five photons and the same rate γ. Solid lines in both the main panel and upper inset correspond to propagation $1 \to 2$; dashed lines in both the main panel inset correspond to propagation $2 \to 1$. In the main panel, propagation through each part occurs during the interval $3\gamma t$; for the upper panel, propagation through each part occurs during the interval $0.5\gamma t$. Lower panel shows the photon number distribution of the output state for propagation $1 \to 2$ depicted in the main panel.

Despite its seemingly idealized character, the scheme with Kraus operators, Eq. (12), can be realized, for example, with nonlinear coherent loss (NCL) described by the Lindblad operators

$$L_j = a(a^\dagger a - m_j), \quad j = 1, 2, \tag{13}$$

m being a positive integer number [37].

It is interesting that the regime of optical isolation with the device described by the Lindblad operators, Eq. (13), functions also with classical inputs. An example of such functioning is shown in Fig. 2. The main panel of Fig. 2 shows how the average number of photons behaves for the input at the part with $m_1 = 4$ (solid line) and output at the part with $m_2 = 2$. Dashed lines show the dynamics of the average number of photons for propagation in the opposite direction. The lower inset shows that the output state for propagation $1 \to 2$ is non-classical, being a mixture of the vacuum with the two-photon Fock state.

Another interesting feature of the Eq. (13) scheme is that non-reciprocity can be quite pronounced even far from the asymptotic regime, i.e., when the state of the mode is far from the one given by the condition $L_j\rho = 0$. This situation is illustrated in the upper panel in Fig. 2. Actually, this feature makes it feasible looking for practical realization of non-reciprocity with designed nonlinear loss of the considered kind. Indeed, close to the stationary state satisfying $L_j\rho = 0$, the dynamics resulted from nonlinear loss is rather slow and can be easily disrupted by common single-photon loss, unavoidable in realistic systems [24,25].

5. TOWARD PRACTICAL NON-RECIPROCITY WITH NONLINEAR DISSIPATION

As already mentioned, practical realization of the dissipative coupling between waveguides is rather simple to achieve, for

example, by laser-writing single-mode waveguides in glass [24,25,32–34], or fabricating planar structures as described in Appendix A (and one might mention that waveguide writing in borosilicate glass has become a very versatile photonic instrument for modeling a plethora of exotic physical effects (see, for example, Refs. [34,38]). Designing nonlinear loss is more difficult and involved. Some schemes were suggested and experimentally demonstrated with trapped ions and atoms, nanomechanical resonators, superconducting microwave circuits, nonlinear Kerr resonators, etc. [39–44]. To demonstrate the way of experimental realization of reciprocity breaking purely by designed nonlinear loss, here we consider a recently suggested scheme with self-Kerr nonlinear waveguides that implements the dissipative coupling scheme depicted in Fig. 1(a) [24,25,45]. This scheme allows to produce two-photon loss or NCL of the kind given by Eq. (13) for $m_j = 1$ combined with two-photon loss for the essentially single-mode device.

Dynamics of the single-mode system considered in Refs. [24,25] is described by the following master equation:

$$\frac{d}{dt}\rho = \sum_{j=0}^{2} \gamma_j (2L_j \rho L_j^\dagger - \rho L_j^\dagger L_j - L_j^\dagger L_j \rho), \qquad (14)$$

where $L_0 = a$ describes common single-photon loss; $L_1 = a^2$ describes two-photon loss, and $L_2 = a(a^\dagger a - 1)$ describes so called NCL [37]; $\gamma_{0,1,2}$ are the corresponding loss rates.

First, let us show that the bipartite system composed of the parts described by master Eq. (14) with different sets of decay rates γ_j can lead to asymptotic breaking of reciprocity. To that end, we assume that for the first part, we have $\gamma_{0,2} = 0$, $\gamma_1 = \gamma$, and for the second part, we have $\gamma_{0,1} = 0$, $\gamma_2 = \gamma$ in Eq. (14), i.e., we have only two-photon loss in the first part and only NCL in the second part of our device. Two-photon loss does not affect states in the subspace of single and zero photon states. Asymptotically, two-photon loss drives an initial state with the number of photons much larger than unity toward a mixed single-photon state with one-half photons on average [23,46]. The NCL described by L_2 also does not affect states in the subspace of single and zero photon states. But asymptotically, it drives an initial state with the number of photons much larger than unity toward the single-photon state [24,37]. So, for the initial coherent state with the average number of photons much larger than unity, the bipartite system will produce asymptotically the state with 1/2 photon on average for $1 \to 2$ propagation, and the single-photon state for propagation in the opposite direction.

Figure 3(b) shows that reciprocity is broken for such a system also for a finite time even in the regime when the system's state is far from the stationary state. For the simulation, we have taken that the system is also subject to common single-photon loss, and that two-photon loss is present also in the second part of the device (which corresponds to the realistic three-waveguide scheme [25,45]). So, for the first part, we have taken $\gamma_0 = \gamma_1 = \gamma$, $\gamma_2 = 0$; for the second part, we have taken $\gamma_j = \gamma$, $\forall j$. The initial state is taken to be the coherent one with amplitude 20. One can see from Fig. 3(b) that the average number of photons at outputs is different, and the photon number distributions of output states [shown in the inset in (b)] are also quite different. Both output states are sub-Poissonian, but for $1 \to 2$ propagation, the state is considerably more photon-number squeezed, with Mandel parameter $Q \approx -0.7$, whereas in the opposite direction, $Q \approx -0.5$.

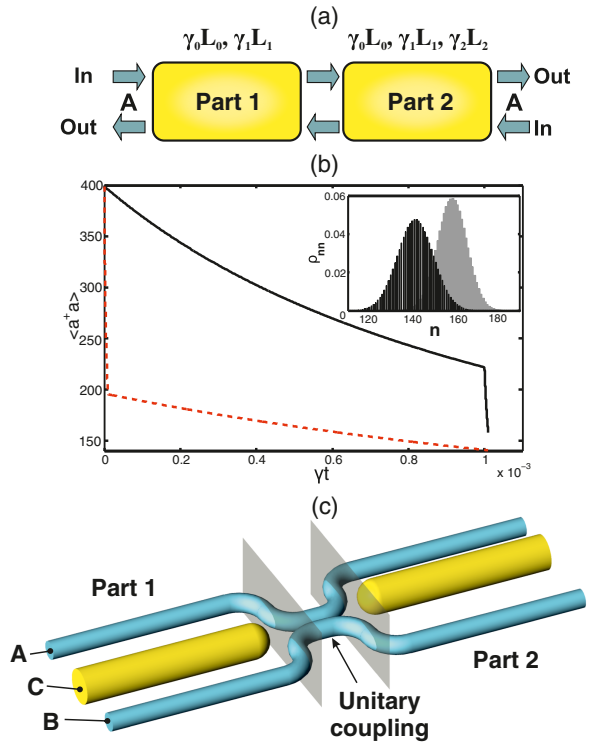

Fig. 3. (a) Scheme of the single-mode bipartite non-reciprocal device described by Eq. (14). (b) Dynamics of the average number of photons for the structure schematically depicted in (a). The solid line corresponds to propagation $1 \to 2$, and dashed line corresponds to propagation in the opposite direction. For part 1, the dynamics is described by master Eq. (14) with decay rates $\gamma_0 = \gamma_1 = \gamma$, $\gamma_2 = 0$. For part 2, the decay rates are $\gamma_{0,1,2} = \gamma$. The unitary transformation between the two parts is supposed to leave the collective mode state unchanged. The initial state at each input is taken as the coherent state of the corresponding "stationary" collective mode with amplitude $\alpha = 20$. The inset shows the output state photon number distribution, ρ_{nn}, for propagation $1 \to 2$ (thick gray bars) and for propagation in the opposite direction, $2 \to 1$ (thin black bars). (c) Example of bipartite nonlinear loss scheme for realizing non-asymptotic breaking of reciprocity by single-mode nonlinear loss. Two self-Kerr nonlinear waveguides are coupled to the third waveguide, but not to each other. The third waveguide is designed to have excess loss. In part 1, the third waveguide is coupled symmetrically to waveguides A and B, realizing two-photon loss. In part 2, the coupling is asymmetric, realizing both two-photon loss and nonlinear coherent loss (NCL). We assume unitary coupling between parts 1 and 2, allowing for lossless transformation of collective mode $\tilde{A}_1$ to collective mode $\tilde{A}_2$ and vice versa.

The single-mode device analyzed above can be realized with the waveguide arrangement schematically shown in Fig. 3(c). The device consists of three parts: parts 1 and 2 realize different kinds of nonlinear loss by the dissipative coupling scheme shown in Fig. 1(a). The symmetric coupling between the side self-Kerr nonlinear waveguides and the lossy central one allows to realize the two-photon loss of the collective mode $A_1 \propto a_1 - b_1$, where a_1, b_1 are the modes guided in corresponding waveguides. Mode A_1 would be a stationary mode of part 1

in absence of nonlinearity and uncorrelated single-photon loss. In part 2, the coupling is asymmetric, so NCL arises described by Lindblad operator L_2 in addition to the two-photon loss for collective mode $A_2 \propto \delta a_2 - b_2$, parameter δ describing the coupling asymmetry [24,37]. Notice that for initial states with large numbers of photons, on the initial stage of dynamics (i.e., when the average number of photons still remains large), NCL dominates two-photon loss, making its influence on photon number dynamics negligible even though the loss rates are close in value [25]). The third part connecting parts 1 and 2 in Fig. 3(a) provides for the effectively single-mode operation of the device transforming collective mode A_1 into A_2 and vice versa. Initially, one should also excite only A_1 for propagation $1 \to 2$, and A_2 from propagation in the opposite direction.

Notice that to demonstrate non-reciprocity, one might simplify the setup in Fig. 3(c), getting rid of the central unitary coupled part, i.e., leaving only two conjoined nonlinear dissipative couplers as in Fig. 1(d). But the single modality of the operation would be lost, and both linear (considered in Section 3) and nonlinear effects of reciprocity breaking would be combined.

6. BREAKING RECIPROCITY BY DEPHASING

We have already shown with examples of both linear and nonlinear dissipative dynamics that dissipative systems possessing several stationary states can break reciprocity. Now let us consider another example of a quite simple and widespread (actually, even virtually ubiquitous) kind of dissipative dynamics with several (and possibly even infinite number of) stationary states that can also break reciprocity. Also, this reciprocity violation cannot be captured by a simple classical criterion implementing the amplitude scattering matrix Eq. (7).

This kind of dissipation is dephasing [47]. The essence of it is as follows. The dephasing with respect to some orthogonal basis $\{|\psi_j\rangle\}$ (i.e, $\langle\psi_k|\psi_j\rangle = \delta_{kj}$) means that asymptotically, any state is transformed to a state with only diagonal components in this basis:

$$\rho = \sum_{\forall j,k} c_{jk}|\psi_j\rangle\langle\psi_k| \to \bar{\rho} = \sum_{\forall j} c_{jj}|\psi_j\rangle\langle\psi_j|, \qquad (15)$$

where coefficients c_{jk} describe the representation of the state density matrix in the basis $\{|\psi_j\rangle\}$. Transformation Eq. (15) is realized by the Kraus operators $D_j = |\psi_j\rangle\langle\psi_j|$, and any state commuting with all these Kraus operators is stationary.

It is easy to see that a bipartite system with each part performing dephasing with respect to different bases breaks reciprocity. Indeed, let us take that the jth part dephases the input state with respect to the basis $\{|\psi_k^{(j)}\rangle\}$, and at least for some j and k, one has $\langle\psi_k^{(1)}|\psi_j^{(2)}\rangle \neq 0$. Then, the corresponding Kraus operators $D^{(1)k}$ and $D^{(2)j}$ do not commute and the dynamics is not reciprocal.

Physically, realization of single-mode dephasing in different bases is not simple and involves state transformation corresponding to transition to the different bases. However, reciprocity breaking can be realized conjoining unitary and feasible dephasing parts. Dephasing in the energy basis is quite simply realized by random fluctuation of frequency, or, equivalently, by inducing random fluctuation of modal phase [47]. This kind of dephasing is quite usual for solid-state qubits, such as, for example, quantum dots, and is a common reason for decoherence. Curiously, such dephasing was shown to enable non-reciprocal state transfer between qubits [48,49]. Let us show how it is possible to break reciprocity in propagation of correlations by a bipartite system consisting of a simple 50/50 beam splitter and the energy dephaser.

We take a two-mode bipartite system as shown in Fig. 4(a). Part 1 is a beam splitter performing the following standard transformation:

$$a_{\text{out}} = \frac{1}{\sqrt{2}}(a_{\text{in}} + ib_{\text{in}}), \quad b_{\text{out}} = \frac{1}{\sqrt{2}}(ia_{\text{in}} + b_{\text{in}}). \qquad (16)$$

Part 2 is the dephaser in the energy basis. The way to realize this setup in practice is depicted in Fig. 4(b). The dephaser is realized by phase randomizers on the output modes acting on a modal annihilation operator x in the following way: $x \to e^{-i\phi}x$. So, any density matrix ρ dephases in the following way given by Eq. (15):

$$\rho = \sum_{m,n} \rho_{mn}|m\rangle\langle n| \to \frac{1}{2\pi}\int_0^{2\pi} d\phi \sum_{m,n} \rho_{mn} e^{i(n-m)\phi}|m\rangle\langle n|$$

$$= \sum_m \rho_{mm}|m\rangle\langle m|.$$

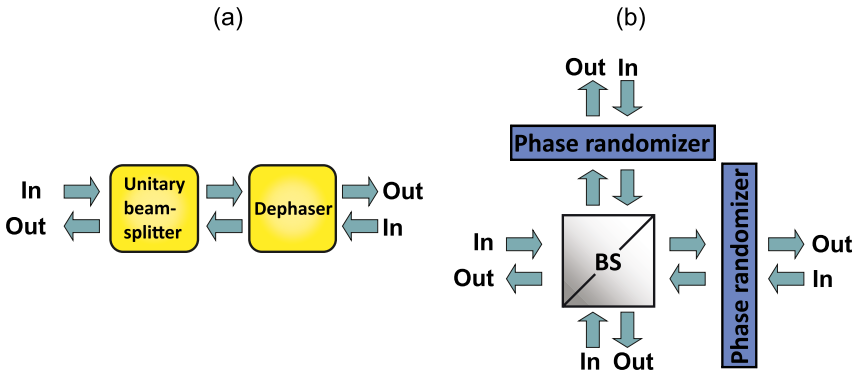

Fig. 4. (a) Scheme of bipartite device for breaking reciprocity by unitary beam splitting and dephasing. (b) Example of the practical realization of the scheme in (a) with phase randomizers for performing dephasing.

Similarly, one can introduce energy dephazing for any multimodal state by phase-randomizing each mode [as shown for our two-modal scheme in Fig. 4(b)].

Let us consider the following pure input state:

$$\rho_{\rm in} = |\psi\rangle\langle\psi|, \quad |\psi\rangle = x|1_a\rangle|0_b\rangle + \sqrt{1-x^2}|0_a\rangle|1_b\rangle, \tag{17}$$

where vector $|n_x\rangle$ is the Fock state of mode x with n_x photons, and a real x satisfies $|x| \le 1$.

Now, as discussed in Section 2, let us consider an observable $P = \lambda a^\dagger b + \lambda^* b^\dagger a$, where λ is a scalar parameter. It is easy to see that the value of this observable for the initial state, Eq. (17), is

$$p = {\rm Tr}\{P\rho_{\rm in}\} = (\lambda + \lambda^*)x\sqrt{1-x^2}.$$

For propagation $1 \to 2$, we have from Eqs. (16) and (17) $\overrightarrow{p} = 0$. For propagation $2 \to 1$, we have

$$\overleftarrow{p} = \frac{i}{2}(\lambda - \lambda^*)(1-2x^2).$$

So, according to the definition given by Eqs. (4) and (5), for $\lambda \neq \lambda^*$ and $|x| \neq 1/\sqrt{2}$, our device is indeed breaking reciprocity. In our case, modal correlations are non-reciprocally transmitted through our bipartite device. Notice that the classical definition, Eq. (2), cannot work for the case. For the initial state, Eq. (17), modal amplitudes are zero.

7. ASYMMETRIC DISSIPATIVELY COUPLED DISTRIBUTOR

Finally, let us demonstrate how purely dissipative coupling might serve for building an asymmetric optical "distributor," i.e., a device that asymmetrically transfers modal energy between modes depending on the initial excitation. We consider a bipartite structure with each part having three physical modes A, B, C, where dissipative coupling is only between modes A, B and B, C (which makes the structure feasible to fabricate using a planar arrangement of strongly coupled low-loss waveguides A, B, C and high-loss waveguides D as shown in Fig. 5(a); such a structure is a simple generalization of the ones discussed in Appendix A).

Each part of our bipartite setup is described by the following master equation ($j = 1, 2$):

$$\frac{d}{dt}\rho = \sum_{x=AB,BC} \gamma_{x,j}(2L_{x,j}\rho L_{x,j}^\dagger - \rho L_{x,j}^\dagger L_{x,j} - L_{x,j}^\dagger L_{x,j}\rho), \tag{18}$$

where γ_{xj} are corresponding loss rates, and the Lindblad operators are given by

$$L_{AB,j} = a + y_j b, \quad L_{BC,j} = b + z_j c, \tag{19}$$

where y_j, z_j are the asymmetry parameters. We consider only propagation from part 1 to part 2.

To uncover specifics of the non-reciprocal field transfer among modes A, B, and C performed by the device shown in Fig. 5(a), let us consider first the asymptotic regime when the single-photon uncorrelated loss is absent and the lengths of both parts are sufficiently large for transition to the stationary state. From Eq. (18), one gets the following relation between input and output values of the modal amplitudes:

$$\begin{bmatrix} \langle a_{\rm out}\rangle \\ \langle b_{\rm out}\rangle \\ \langle c_{\rm out}\rangle \end{bmatrix} = \mathbf{S}_j \begin{bmatrix} \langle a_{\rm in}\rangle \\ \langle b_{\rm in}\rangle \\ \langle c_{\rm in}\rangle \end{bmatrix},$$

$$\mathbf{S}_j = \frac{1}{F_j}\begin{bmatrix} (y_j z_j)^2 & -y_j z_j^2 & -y_j z_j \\ -y_j z_j^2 & z_j^2 & -z_j \\ -y_j z_j & -z_j & 1 \end{bmatrix}, \tag{20}$$

where $F_j = z_j^2(1+y_j^2)+1$. From Eq. (20), one has

$$\left|\frac{[\mathbf{S}_1\mathbf{S}_2]_{12}}{[\mathbf{S}_1\mathbf{S}_2]_{21}}\right| = \left|\frac{y_1}{y_2}\right|, \quad \left|\frac{[\mathbf{S}_1\mathbf{S}_2]_{23}}{[\mathbf{S}_1\mathbf{S}_2]_{32}}\right| = \left|\frac{z_1}{z_2}\right|,$$

$$\left|\frac{[\mathbf{S}_1\mathbf{S}_2]_{13}}{[\mathbf{S}_1\mathbf{S}_2]_{31}}\right| = \left|\frac{y_1 z_1}{y_2 z_2}\right|. \tag{21}$$

So, whereas for our scheme, it is hardly possible to realize an ideal circulator (which provides for unidirectional transfer, i.e., $A \to B$, $B \to C$, and $C \to A$) with the device in Fig. 5(a), nevertheless, energy transfer between the waveguides is strongly asymmetric.

In Figs. 5(b)–5(d), we show an example of asymmetric field distribution for the bipartite structure as given by Eqs. (18) and (19) with the all equal decay rates $\gamma_{x,j} = \gamma, \forall x,\ j$, and mirrored asymmetry parameters in different parts, $y_1 = -z_2 = -0.9$, $y_2 = -z_1 = -0.1$. In Figs. 5(b)–5(d), solid, dashed, and dashed-dotted lines correspond to the modal amplitudes of modes A, B, and C, respectively, and these figures correspond to the initial coherent excitation with the unit amplitude of modes A, B, and C with the vacuum of the other two modes. The transformation of the modal amplitudes at the end of part 2 as shown in Figs. 5(b)–5(d) is described by the following scattering matrix:

$$\mathbf{S}_1\mathbf{S}_2 = \begin{bmatrix} 0.0075 & 0.0070 & -0.0529 \\ 0.0692 & 0.0669 & -0.5306 \\ -0.0768 & -0.0743 & 0.5897 \end{bmatrix}. \tag{22}$$

Matrix Eq. (22) shows about 20 dB asymmetry in power transfer between waveguides A and B, and B and C. Notice that due to strong coupling asymmetry, even for the interaction time much exceeding the inverse decay rate γ^{-1}, the dynamics shown in Figs. 5(b)–5(d) is still not close to the asymptotic regime.

The dynamics shown in Figs. 5(b)–5(d) demonstrates another curious feature, namely, that the asymmetry in field distribution does not always require and is not always connected to breaking of reciprocity (for a discussion, see, for example, Ref. [4]). Each part of the structure depicted in Fig. 5(a) does break reciprocity by itself. However, for example, part 1 by itself provides for quite asymmetric field propagation from waveguide A to waveguide B, and from waveguide C to waveguide B. Excitation of waveguide A creates strong excitation of mode B, whereas excitation mode C leaves mode B non-excited. It is interesting to notice that an asymmetric but reciprocal field distributor was suggested in Ref. [34] for a dissipatively coupled chain of waveguides. There, excitation was shown to spread either to the left waveguide chain or to the right one in dependence on the excitation of the control waveguide.

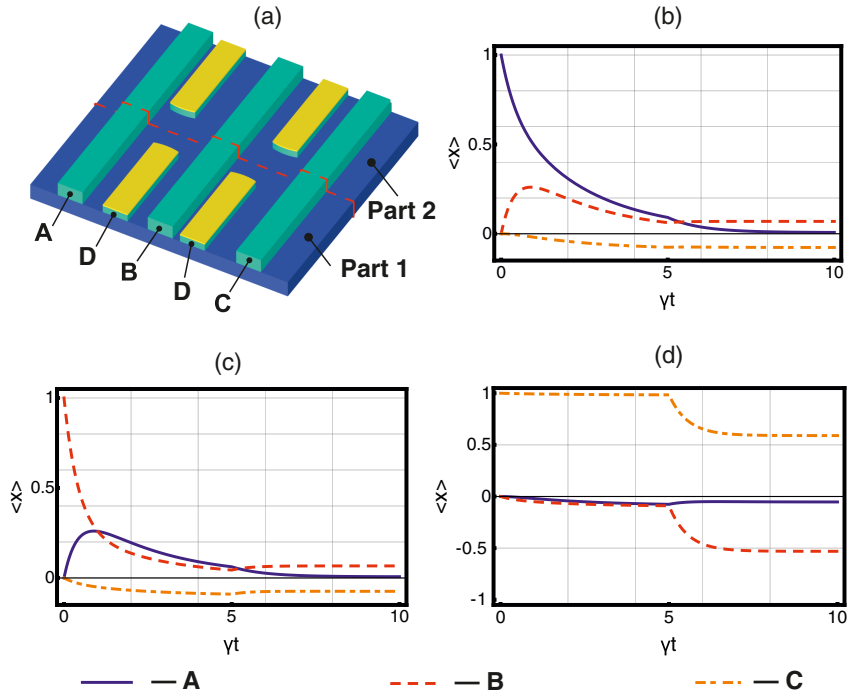

Fig. 5. (a) Scheme of bipartite three-mode dissipatively coupled distributor. We consider only propagation $1 \to 2$. (b)–(d) Dynamics of modal amplitudes as given by Eqs. (18) and (19) with decay rates $\gamma_{x,j} = \gamma, \forall x,\ j$, and asymmetry parameters $y_1 = -z_2 = -0.9$, $y_2 = -z_1 = 0.1$. The border between the parts corresponds to $\gamma t = 5$. In (b)–(d) solid, dashed, and dashed-dotted lines correspond to the modal amplitudes of the modes in waveguides $x = A,\ B,\ C$, and (b)–(d) correspond to the initial coherent excitation with the unit amplitude of the modes of waveguides A, B, and C with the vacuum of the other two modes.

8. CONCLUSION

Here we have shown that dissipatively coupled systems can break reciprocity even without simultaneous conjoining unitary and dissipative coupling. Even for linear systems, dynamics corresponding to different dissipative coupling is not commutative. This can give rise to practical linear optical diode devices providing for unidirectional field propagation for certain classes of input states. We outline the way to fabricate such devices using laser-written waveguides in glass or a generic integration platform on the basis of such standard materials as InP (in Appendix A, we outline practical ways to create such planar integrated structures).

We show also that designed nonlinear loss enables one to create a single-mode optical insulator. We demonstrate the way to do that with NCL, and show it is possible to achieve single-mode non-asymptotic breaking of reciprocity with a practically realizable system of waveguides with self-Kerr nonlinearity. Such a system can realize both two-photon loss and NCL, able asymptotically to produce a single-photon state from the initial coherent state. We also show that dephasing is able to induce non-reciprocity, and demonstrate non-reciprocity of correlation transfer with a simple example of a bipartite system including a beam splitter and a dephaser. We demonstrate an example of a non-reciprocal optical distributor in a three-mode system with purely dissipative coupling.

APPENDIX A: POSSIBILITIES FOR PRACTICAL IMPLEMENTATION

In this appendix, we propose several options for practical realization of dissipative coupling that can be used to construct the schemes discussed above (i.e., constitute components of the bipartite setups discussed there). The suggested solutions use a mature COBRA/Smart Photonics InP integration platform [35], which features a large set of standard building blocks, and thus can be used to integrate the dissipative couplers in more complex circuits.

The suggested dissipative coupler consists of three parallel single-mode waveguides A, B, and C, where C corresponds to the common loss reservoir as shown in Fig. 1(a). Waveguide C is placed between A and B, and has excessive loss Γ compared to them. Light coupling occurs in waveguide pairs A–C and C–B.

Platform description. In the selected integration platform [35], there are two types of waveguides: active and passive; see Fig. 6. *Passive* refers to a lattice-matched InGaAsP material that is transparent in the C band (1530–1565 nm). It is used as a waveguiding layer with InP as upper and lower cladding layers with a lower refractive index. *Active* is a quantum well (QW)-based structure that uses quaternary InGaAsP material with a composition chosen to have an emission wavelength and bandgap around 1550 nm. This leads to the presence of absorption at this wavelength and provides a means to create a controlled amount of excess loss in waveguide C.

We have considered three possible ways of achieving excess loss in the middle waveguide, shown in Fig. 6.

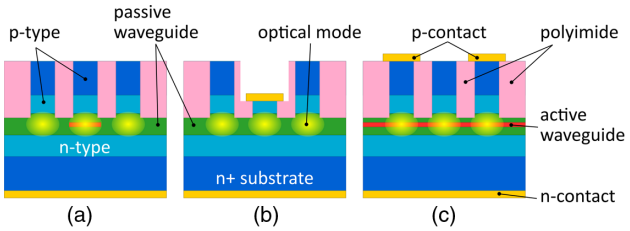

Fig. 6. Possible implementations of the dissipative coupler. (a) Active unbiased waveguide, (b) passive waveguide in isolation cross section with metal, and (c) active waveguides with applied bias. In each cross section, two side waveguides and a middle waveguide with extra loss are shown.

Unbiased active sections. This option is shown in Fig. 6(a). The middle waveguide is an active waveguide with high absorption at 1550 nm if unbiased [50]. This is the most natural solution considering the absorption spectra of active and passive waveguides. However, taking into account the required distance between waveguides (below 3 μm), the reliable integration of such narrow active stripes by passive regrowth is not possible with the current fabrication flow.

Passive waveguides with metal. This option is shown in Fig. 6(b). The middle waveguide is fabricated in the isolation cross section, in which the strongly conductive part of the top p-type cladding layer is removed. If we add the metal on top of this waveguide, it will overlap with the optical mode and cause extra losses. This option does not require any electrical signals to be applied to the coupler. However, there is no possibility of tuning the excess loss on the middle waveguide.

Active waveguides with applied bias. This option is shown in Fig. 6(c). All three waveguides are fabricated in the active cross section, and the two side waveguides have metal contacts connected on top of them. By applying reverse bias voltage or pump current to these metal pads, one can control the absorption in the QW layer, and thus tune the amount of excess loss in the middle waveguide. This scheme allows some tunability, but requires an active driving electronic to be permanently connected. Similar to the first option, a small distance between waveguides means that the opening between the metal stripes will be 3–4 μm, which is on the limit of the fabrication technology.

APPENDIX B: APPEARANCE OF DISSIPATIVE COUPLING

Here we show how dissipative coupling arises in the system of unitary coupled waveguides shown in Fig. 1(a) in the presence of strong linear loss in the middle waveguide, C, along the lines outlined, for example, in Ref. [24]. The system of three coupled single-mode waveguides shown in Fig. 1(a) is described by the following master equation:

$$\frac{d}{dt}\rho_{all} = i[H, \rho_{all}] + \Gamma(2c\rho_{all}c^\dagger - \rho_{all}c^\dagger c - c^\dagger c\rho_{all}), \tag{B1}$$

where the Hamiltonian H describes unitary interaction between modes:

$$H = c^\dagger(g_a a + g_b b) + (g_a a^\dagger + g_b b^\dagger)c. \tag{B2}$$

In Eqs. (B1) and (B2), x and $x^\dagger$, $x = a, b, c$ are annihilation and creation operators of the waveguide modes, respectively; Γ is the loss rate of mode C, and $g_{a,b}$ are interaction constants describing coupling strengths of modes A and B with mode C. For simplicity, let us take $g_{a,b}$ to be real, and $|g_a g_b| > 0$.

Next, let us suppose that the loss rate Γ is so large that the state of central mode C quickly goes to the vacuum during the time when the states of modes A and B are only weakly changed. Then, mode C can be adiabatically eliminated, which results in the following reduced master equation only for the state of modes A and B [47]:

$$\frac{d}{dt}\rho = \gamma\big(2(a+\delta b)\rho(a^\dagger + \delta b^\dagger) - \rho(a^\dagger + \delta b^\dagger)(a+\delta b) - (a^\dagger + \delta b^\dagger)(a+\delta b)\rho\big), \tag{B3}$$

where the loss rate is $\gamma = 4g_a^2/\Gamma$, and the asymmetry parameter is $\delta = g_b/g_a$. Equation (B3) is the one describing each part of the device considered in Section 3.

Funding. European Regional Development Fund (Open Innovation Photonic ICs project (PROJ-00315)); European Commission (project PhoG 820365, NATO SPS—G5860).

Acknowledgment. The authors (D.M. and I.P.) gratefully acknowledge support from the EU project PhoG and the NATO project; D.P. acknowledges the Dutch Stimulus OPZuid Programme through the Open Innovation Photonic ICs Project. The authors thank Prof. K. Williams for useful criticism and fruitful discussion.

Disclosures. The authors declare no conflicts of interest.

Data availability. No data were generated or analyzed in the presented research.

REFERENCES

1. D. Pozar, *Microwave Engineering*, 4th ed. (Wiley, 2011).
2. R. J. Potton, "Reciprocity in optics," Rep. Prog. Phys. **67**, 717–754 (2004).
3. M. V. de Hoop and A. T. de Hoop, "Wave-field reciprocity and optimization in remote sensing," Proc. R. Soc. A **456**, 641–682 (2000).
4. C. Caloz, A. Alù, S. Tretyakov, D. Sounas, K. Achouri, and Z.-L. Deck-Léger, "Electromagnetic nonreciprocity," Phys. Rev. Appl. **10**, 047001 (2018).
5. S. V. Kutsaev, A. Krasnok, S. N. Romanenko, A. Y. Smirnov, K. Taletski, and V. P. Yakovlev, "Up-and-coming advances in optical and microwave nonreciprocity: from classical to quantum realm," Adv. Photon. Res. **2**, 2000104 (2021).
6. R. Ma, S. Reniers, Y. Shoji, T. Mizumoto, K. Williams, Y. Jiao, and J. van der Tol, "Integrated polarization-independent optical isolators and circulators on an InP membrane on silicon platform," Optica **8**, 1654–1661 (2021).
7. D. Sounas and A. Alù, "Non-reciprocal photonics based on time modulation," Nat. Photonics **11**, 774–783 (2017).
8. T. T. M. van Schaijk, D. Lenstra, K. A. Williams, and E. A. J. M. Bente, "Model and experimental validation of a unidirectional phase modulator," Opt. Express **26**, 32388–32403 (2018).
9. Y. Shi, Z. Yu, and S. Fan, "Limitations of nonlinear optical isolators due to dynamic reciprocity," Nat. Photonics **9**, 388–392 (2015).
10. A. Mahmoud, A. Davoyan, and N. Engheta, "All-passive nonreciprocal metastructure," Nat. Commun. **6**, 8359 (2015).
11. A. Li and W. Bogaerts, "Reconfigurable nonlinear nonreciprocal transmission in a silicon photonic integrated circuit," Optica **7**, 7–14 (2020).

12. G. Y. Slepyan and A. Boag, "Quantum nonreciprocity of nanoscale antenna arrays in timed Dicke states," Phys. Rev. Lett. **111**, 023602 (2013).
13. A. Rosario Hamann, C. Müller, M. Jerger, M. Zanner, J. Combes, M. Pletyukhov, M. Weides, T. M. Stace, and A. Fedorov, "Nonreciprocity realized with quantum nonlinearity," Phys. Rev. Lett. **121**, 123601 (2018).
14. N. Nefedkin, M. Cotrufo, A. Krasnok, and A. Alù, "Dark-state induced quantum nonreciprocity," Adv. Quantum Technol. **5**, 2100112 (2022).
15. E. Verhagen and A. Alù, "Optomechanical nonreciprocity," Nat. Phys. **13**, 922–924 (2017).
16. T. Ozawa, H. M. Price, A. Amo, N. Goldman, M. Hafezi, L. Lu, M. C. Rechtsman, D. Schuster, J. Simon, O. Zilberberg, and I. Carusotto, "Topological photonics," Rev. Mod. Phys. **91**, 015006 (2019).
17. L. Lu, J. Joannopoulos, and M. Soljačić, "Topological photonics," Nat. Photonics **8**, 821–829 (2014).
18. J. Koch, A. A. Houck, K. L. Hur, and S. M. Girvin, "Time-reversal-symmetry breaking in circuit-QED-based photon lattices," Phys. Rev. A **82**, 043811 (2010).
19. X. Huang, C. Lu, C. Liang, H. Tao, and Y. Liu, "Loss-induced nonreciprocity," Light Sci. Appl. **10**, 30 (2021).
20. A. Metelmann and A. A. Clerk, "Nonreciprocal photon transmission and amplification via reservoir engineering," Phys. Rev. X **5**, 021025 (2015).
21. C. C. Wanjura, M. Brunelli, and A. Nunnenkamp, "Topological framework for directional amplification in driven-dissipative cavity arrays," Nat. Commun **11**, 3149 (2020).
22. L. Mandel and E. Wolf, *Optical Coherence and Quantum Optics* (Cambridge University, 1995).
23. H. Ezaki, E. Hanamura, and Y. Yamamoto, "Generation of phase states by two-photon absorption," Phys. Rev. Lett. **83**, 3558–3561 (1999).
24. D. Mogilevtsev and V. S. Shchesnovich, "Single-photon generation by correlated loss in a three-core optical fiber," Opt. Lett. **35**, 3375–3377 (2010).
25. M. Thornton, A. Sakovich, A. Mikhalychev, J. D. Ferrer, P. de la Hoz, N. Korolkova, and D. Mogilevtsev, "Coherent diffusive photon gun for generating nonclassical states," Phys. Rev. Appl. **12**, 064051 (2019).
26. P. T. Leung and K. Young, "Gauge invariance and reciprocity in quantum mechanics," Phys. Rev. A **81**, 032107 (2010).
27. L. Deák and T. Fülöp, "Reciprocity in quantum, electromagnetic and other wave scattering," Ann. Phys. **327**, 1050–1077 (2012).
28. D. Jalas, A. Petrov, M. Eich, W. Freude, S. Fan, Z. Yu, R. Baets, M. Popovic, A. Melloni, J. Joannopoulos, M. Vanwolleghem, C. Doerr, and H. Renner, "What is—and what is not—an optical isolator," Nat. Photonics **7**, 579–582 (2013).
29. L. Ranzani and J. Aumentado, "Graph-based analysis of nonreciprocity in coupled-mode systems," New J. Phys. **17**, 023024 (2015).
30. T. Gruner and D.-G. Welsch, "Quantum-optical input-output relations for dispersive and lossy multilayer dielectric plates," Phys. Rev. A **54**, 1661–1677 (1996).
31. A. Krasnok, D. Baranov, H. Li, M.-A. Miri, F. Monticone, and A. Alú, "Anomalies in light scattering," Adv. Opt. Photon. **11**, 892–951 (2019).
32. D. N. Biggerstaff, R. Heilmann, A. A. Zecevik, M. Gräfe, M. A. Broome, A. Fedrizzi, S. Nolte, A. Szameit, A. G. White, and I. Kassal, "Enhancing coherent transport in a photonic network using controllable decoherence," Nat. Commun. **7**, 11282 (2016).
33. T. Eichelkraut, S. Weimann, S. Stützer, S. Nolte, and A. Szameit, "Radiation-loss management in modulated waveguides," Opt. Lett. **39**, 6831–6834 (2014).
34. S. Mukherjee, D. Mogilevtsev, G. Slepyan, T. H. Doherty, R. Thomson, and N. Korolkova, "Dissipatively coupled waveguide networks for coherent diffusive photonics," Nat. Commun. **8**, 1909 (2017).
35. L. M. Augustin, R. Santos, E. den Haan, S. Kleijn, P. J. A. Thijs, S. Latkowski, D. Zhao, W. Yao, J. Bolk, H. Ambrosius, S. Mingaleev, A. Richter, A. Bakker, and T. Korthorst, "InP-based generic foundry platform for photonic integrated circuits," IEEE J. Sel. Top. Quantum Electron. **24**, 6100210 (2018).
36. K. Kraus, A. Böhm, J. D. Dollard, and W. H. Wootters, *States, Effects, and Operations Fundamental Notions of Quantum Theory* (Springer, 1983), Vol. **190**.
37. A. Mikhalychev, D. Mogilevtsev, and S. Kilin, "Nonlinear coherent loss for generating non-classical states," J. Phys. A **44**, 325307 (2011).
38. S. Mukherjee, M. Di Liberto, P. Öhberg, R. R. Thomson, and N. Goldman, "Experimental observation of Aharonov-Bohm cages in photonic lattices," Phys. Rev. Lett. **121**, 075502 (2018).
39. J. F. Poyatos, J. I. Cirac, and P. Zoller, "Quantum reservoir engineering with laser cooled trapped ions," Phys. Rev. Lett. **77**, 4728–4731 (1996).
40. A. R. R. Carvalho, P. Milman, R. L. de Matos Filho, and L. Davidovich, "Decoherence, pointer engineering, and quantum state protection," Phys. Rev. Lett. **86**, 4988–4991 (2001).
41. F. Verstraete, M. M. Wolf, and J. Ignacio Cirac, "Quantum computation and quantum-state engineering driven by dissipation," Nat. Phys. **5**, 633–636 (2009).
42. D. Leibfried, R. Blatt, C. Monroe, and D. Wineland, "Quantum dynamics of single trapped ions," Rev. Mod. Phys. **75**, 281–324 (2003).
43. R. Ma, B. Saxberg, C. Owens, N. Leung, Y. Lu, J. Simon, and D. I. Schuster, "A dissipatively stabilized Mott insulator of photons," Nature **566**, 51–57 (2019).
44. P. Rabl, A. Shnirman, and P. Zoller, "Generation of squeezed states of nanomechanical resonators by reservoir engineering," Phys. Rev. B **70**, 205304 (2004).
45. P. de la Hoz, A. Sakovich, A. Mikhalychev, M. Thornton, N. Korolkova, and D. Mogilevtsev, "Integrated source of path-entangled photon pairs with efficient pump self-rejection," Nanomaterials **10**, 1952 (2020).
46. M. Alexanian and S. K. Bose, "Comment on "Generation of phase states by two-photon absorption"," Phys. Rev. Lett. **85**, 1136 (2000).
47. H. Breuer, F. Petruccione, and S. Petruccione, *The Theory of Open Quantum Systems* (Oxford University, 2002).
48. Y. Matsuzaki, V. M. Bastidas, Y. Takeuchi, W. J. Munro, and S. Saito, "One-way transfer of quantum states via decoherence," J. Phys. Soc. Jpn. **89**, 044003 (2020).
49. K. Yamamoto, Y. Ashida, and N. Kawakami, "Rectification in nonequilibrium steady states of open many-body systems," Phys. Rev. Res. **2**, 043343 (2020).
50. D. Pustakhod, K. Williams, and X. Leijtens, "Method for polarization-resolved measurement of electroabsorption," IEEE Photon. J. **10**, 6600611 (2018).